Available online at www.sciencedirect.com
ScienceDirect
International Journal of Heat and Mass Transfer 50 (2007) 1248–1254
International Journal of HEAT and MASS TRANSFER
www.elsevier.com/locate/ijhmt

Effects of entrance region transport processes on free convection slip flow in vertical microchannels with isothermally heated walls

Laxmidhar Biswal [1], S.K. Som, Suman Chakraborty *

Department of Mechanical Engineering, Indian Institute of Technology, Kharagpur 721302, India

Received 24 June 2005; received in revised form 9 September 2006
Available online 28 November 2006

Abstract

Natural convection gaseous slip flows in vertical microchannels with isothermal wall conditions are numerically investigated, in order to analyze the influence of the entrance (developing) region on the overall heat transfer characteristics. A long channel aspect ratio is considered, so as to achieve both hydrodynamically and thermally fully developed conditions at the channel exit. In other words, the flow-field within the microchannel consists of both developing and fully developed regimes. A wide range of Rayleigh number is covered, so that the cases of very short and relatively large entrance lengths can be analyzed in the same unified mathematical framework. With first order velocity and temperature jump conditions at the microchannel walls, local and average Nusselt number values are computed, by invoking the Navier Stokes equation and the energy conservation equation. It is recognized that the micro-scale effects, being associated with the velocity slip and temperature jump conditions, exhibit enhancements in the rate of heat transfer, as compared to the similar macro-scale geometries. The relative enhancements in the average Nusselt number become more prominent for higher values of Knudsen number, whereas this augmentation effect is found to be somewhat arrested at higher values of Rayleigh number. Contrasting features in the heat transfer rate predictions with and without the considerations of the entrance region effects are also carefully noted.

1. Introduction

Microelectromechanical systems (MEMS) based devices find their applications in a wide variety of emerging technologies, ranging from the microactuators, microsensors, microreactors to the microchannel heat sinks and the thermo-mechanical data storage systems, to name a few. Design and optimization of many of these microdevices involve the analysis of gas flows through microfluidic conduits, thereby emphasizing the need for reliable and efficient mathematical models to address the issues of coupled flow physics and heat transfer over the reduced length scales.

The primary challenges associated with the computational analysis of microscale gaseous flows originate from the fact that the flow physics tend to get changed altogether, as one reduces the length scales from the macro domain to the micro domain. The classical continuum hypothesis ceases to work as the distance traversed by molecules between successive collisions (i.e., the mean free path, λ) becomes comparable with the characteristic length scale of the system (D) over which characteristic changes in the transport phenomena are expected to occur. The ratio of these two quantities, known as the Knudsen number ($Kn = \lambda/D$), is an indicator of the degree of rarefaction of the system, which determines the extent of deviation from a possible continuum behaviour (see Fig. 1). For $0 < Kn < 0.01$, the flow domain can be treated as a continuum, in which the Navier Stokes equation in conjunction with the no-slip wall boundary conditions become applicable. On the other extreme, when $Kn > 10$, the flow becomes free

* Corresponding author. Tel.: +91 3222 282990; fax: +91 3222 282278.
E-mail address: suman@mech.iitkgp.ernet.in (S. Chakraborty).
[1] On leave from Delphi Tech Center India, 5th Floor, Innovator, ITPL, Whitefield Road, Bangalore 560 037, India.

0017-9310/$ - see front matter © 2006 Elsevier Ltd. All rights reserved.
doi:10.1016/j.ijheatmasstransfer.2006.09.025

Nomenclature

a	channel aspect ratio $\left(\frac{H}{D}\right)$
c_p	specific heat at constant pressure, J/kg K
D	width of channel, m
g	gravitational acceleration, m/s^2
H	height of channel, m
h	local heat transfer coefficient $\left(-k\frac{\mathrm{d}T}{\mathrm{d}x}\Big\|_{\mathrm{w}} \cdot \frac{1}{T_{\mathrm{w}}-T_{\infty}}\right)$
k	thermal conductivity, W/m K
Kn	Knudsen number $\left(\frac{\lambda}{D}\right)$
Nu	local Nusselt number $\left(\frac{h_y D}{k}\right)$
$\overline{Nu}$	average Nusselt number
p	pressure, Pa
Q'	non-dimensional volume flow rate
Ra	Rayleigh number based on ambient properties
u	velocity component in the x-direction, m/s
v	velocity component in the y-direction, m/s
v_{avg}	average velocity in the y-direction, m/s
v_{s}	wall-slip velocity, m/s
T	temperature, K
T_{∞}	temperature of free stream air, K
T_{w}	temperature of wall, K
y_{eth}	thermal entrance length, m
Y_{eth}	non-dimensional thermal entrance length $\left(\frac{y_{\mathrm{eth}}}{H}\right)$

Greek symbols

β	coefficient of thermal expansion, K^{-1}
θ	non-dimensional temperature $\left(\frac{T-T_{\infty}}{T_{\mathrm{w}}-T_{\infty}}\right)$
θ_{b}	non-dimensional bulk fluid temperature
μ	dynamic viscosity, kg/m s
ρ	density, kg/m^3
γ	ratio of specific heats $\left(\frac{c_p}{c_v}\right)$
λ	molecular mean free path, m
ρ_{∞}	density of free stream air, kg/m^3
σ_{T}	thermal accommodation coefficient
σ_{v}	tangential accommodation coefficient

Subscripts

m	value at mean temperature $(T_{\mathrm{w}}+T_{\infty})/2$
w	wall
∞	free stream or inlet condition

molecular in nature, because of negligible molecular collisions. The range of Kn spanning from 0.01 to 0.1 is known as the slip flow regime, over which the no-slip boundary condition becomes invalid, although continuum conservation equations can still be used to characterize the bulk flow. However, over the Kn range of 0.1–1 (the so called transitional regime), the continuum hypothesis progressively ceases to work altogether, thereby necessitating a shift of paradigm from the continuum-based modeling to particle-based modeling. Although this classification is based on empirical information and the strict demarcating limits between the different flow regimes may depend on the specific problem geometry [1–3], it essentially offers with a qualitative criterion based on which appropriate mathematical models can be chosen for the thermo-fluid analysis, consistent with the underlying physical picture. In this context, it is also important to re-iterate that in micro-scale gas flows, thermodynamic equilibrium may not prevail at the fluid–solid interface. Accordingly, a finite velocity slip and temperature jump may need to be accounted for at the fluid–solid interface [1–6]. Depending on the degree of rarefaction of gaseous flows in micro-scale geometries, appropriate physics needs to be incorporated in the mathematical model to accommodate these effects. It has been well established by various researchers [2,3,7] that the traditional Navier Stokes equations, coupled with velocity slip and temperature jump conditions at the fluid–solid interface, can simulate gaseous flows in micro-scales to a high degree of accuracy in the slip flow regimes. For transition and free molecular flow regimes, however, particle based methods such as the Direct Simulation Monte Carlo (DSMC) need to be adopted [1].

Although a vast body of literature exits on the forced convection gas flows in micro-systems, only a few studies have been reported so far on natural convection in vertical microchannels. Appreciating the technological importance of free convective heat transfer in vertical microchannels, Chen and Weng [8] have recently presented analytical solutions for velocity and temperature distribution in fully developed natural convection in an open-ended vertical parallel plate microchannel, by taking the velocity slip and temperature jump effects into account. They have also shown that the effects of rarefaction and fluid-wall interaction are to increase the volumetric transport and to decrease the heat transfer rate. Further, it has been established in their study [8] that for fully developed free con-

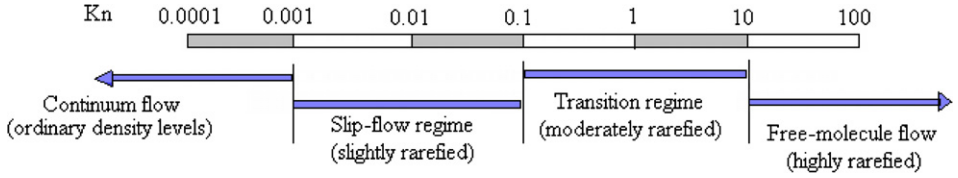

Fig. 1. Gas flow regimes based on Knudsen number.

vection flows with symmetrically heated walls, the Nusselt number turns out to be zero. Such conclusions, however, have been arrived at by neglecting the momentum and heat transfer characteristics in the developing region of the microchannel. On the other hand, in reality, it is expected that the influences of the developing region are likely to alter the free convection heat transfer characteristics in a vertical microchannel to a significant extent. The underling implications might appear to be somewhat intuitive in nature, but are by no means obvious, primarily because of an interesting and non-trivial interplay between the boundary layer growth in the developing region and the micro-scale effects manifested through wall slippage and temperature jump conditions at the gas-solid interface. The situation gets further complicated by the fact that the thermo-physical properties tend to change significantly with changes in temperature, and cannot be taken as constants for the sake of obtaining closed-form solutions of the associated mathematical problem, at the cost of the practical reliability of the model predictions. To the best of our knowledge, these issues are yet to be comprehensively addressed in the context of free convective heat transfer in vertical microchannels. Aim of the present work, accordingly, is to execute a comprehensive computational study on free convection heat transfer in the entrance region, followed by that in the fully developed region, in long vertical microchannels with constant wall temperature conditions, for different values of Knudsen number and Rayleigh number, by taking the temperature-dependent thermo-physical properties into consideration. Both macro-scale (no-slip and no-jump) and micro-scale situations (slip and jump) are studied and compared, so as to develop a thorough physical understanding of the effects of slip and jump conditions on the developing and the developed flows in the microchannel. Special implications of accommodating the effects of the developing region in the heat transfer analysis are discussed in details and some important conclusions based on the same are finally pinpointed.

2. Mathematical modeling

A vertical parallel plate microchannel, along with the coordinate system adopted to analyze the flow and heat transfer characteristics of the same, is depicted in Fig. 2. The height (H) of the channel is considered to be much larger as compared to its width (D), so as to obtain a fully developed flow in the downstream of the channel. The flow is considered to be two-dimensional. The temperature of the walls of the channel is considered to be uniform at T_w, which is higher than the free stream temperature, T_∞. Accordingly, an upward buoyancy induced flow is generated in the channel. Both ends of the channel are open to the ambient with a temperature of T_∞. The effects of compressibility are neglected in the typical low-speed micro-flows addressed in this study, and only the laminar regimes of flow are considered.

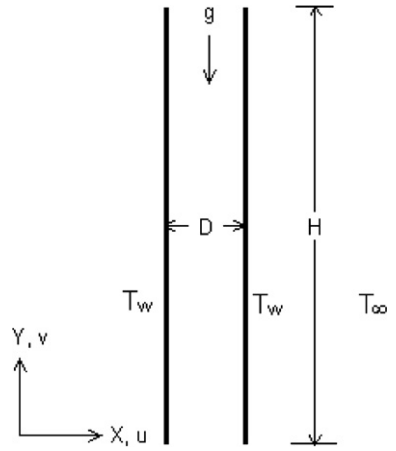

Fig. 2. Geometry of vertical channel and coordinate system with associated velocity components.

The governing equations of mass, momentum and energy conservation for steady, laminar and incompressible flow with temperature dependent thermo-physical properties [9], appropriate to the analysis of the physical problem described as above, can be written as follows:

Continuity

$$\frac{\partial u}{\partial x}+\frac{\partial v}{\partial y}=0 \tag{1}$$

X-momentum

$$\rho\left(u\frac{\partial u}{\partial x}+v\frac{\partial u}{\partial y}\right)=-\frac{\partial p}{\partial x}+\frac{\partial}{\partial x}\left(\mu\frac{\partial u}{\partial x}\right)+\frac{\partial}{\partial y}\left(\mu\frac{\partial u}{\partial y}\right) \tag{2}$$

Y-momentum

$$\rho\left(u\frac{\partial v}{\partial x}+v\frac{\partial v}{\partial y}\right)=-\frac{\partial p}{\partial y}+\frac{\partial}{\partial x}\left(\mu\frac{\partial v}{\partial x}\right)+\frac{\partial}{\partial y}\left(\mu\frac{\partial v}{\partial y}\right)+\rho g\beta(T-T_\infty) \tag{3}$$

Energy

$$u\frac{\partial(\rho c_p T)}{\partial x}+v\frac{\partial(\rho c_p T)}{\partial y}=\frac{\partial}{\partial x}\left(k\frac{\partial T}{\partial x}\right)+\frac{\partial}{\partial y}\left(k\frac{\partial T}{\partial y}\right)+\mu\left[2\left\{\left(\frac{\partial u}{\partial x}\right)^2+\left(\frac{\partial v}{\partial y}\right)^2\right\}+\left(\frac{\partial u}{\partial y}+\frac{\partial v}{\partial x}\right)^2\right] \tag{4}$$

The boundary conditions employed for the solution of Eqs. (1)–(4) are as follows:

Inlet

$$u=0,\ v=v_{\text{avg}}\ \text{(based on the exit mass flow rate)},\quad T=T_\infty \tag{5}$$

Outlet

$$\frac{\partial u}{\partial y}=0,\quad \frac{\partial v}{\partial y}=0,\quad \frac{\partial T}{\partial y}=0 \tag{6}$$

Walls [10]

$$u = 0,\ v_s = \frac{2-\sigma_v}{\sigma_v} KnD \left(\frac{\partial v}{\partial x}\right)_w,$$
$$T_s = T_w + \frac{2-\sigma_T}{\sigma_T}\frac{2\gamma}{\gamma+1} KnD \left(\frac{1}{Pr}\frac{\partial T}{\partial x}\right)_w \quad (7)$$

The Nusselt number, as averaged over the entire channel height, H, is finally evaluated from the solution of the temperature field, as follows [11]:

$$\overline{Nu} = \frac{\bar{h}D}{k_m} \quad (8)$$

where k_m is the thermal conductivity of the gas evaluated at a temperature of $(T_w + T_\infty)/2$, and $\bar{h}$ is the average heat transfer coefficient, defined as

$$\bar{h} = \frac{1}{H}\int_0^H h(y)\mathrm{d}y \quad (8a)$$

In Eq. (8a), h is the local heat transfer coefficient, calculated as

$$h(y) = \frac{1}{T_w - T_\infty}\left(-k\frac{\partial T}{\partial x}\bigg|_w\right) \quad (8b)$$

For numerical solution of the system of governing transport equations, a finite volume method is employed. The resultant systems of discretized linear algebraic equations are solved by using the Stone's Implicit Procedure (SIP) [12]. The SIMPLE [13] algorithm is used for the pressure-velocity coupling, whereas the power-law [13] scheme is used for the convection–diffusion formulations. As an aid for handling non-linearities, suitable under-relaxation parameters are introduced in the iterative scheme, to achieve controlled convergence. A comprehensive grid-independence study is undertaken to determine the appropriate spatial discretization and the iteration convergence criteria to be used. The quantities examined in this study are the maximum magnitudes of the two velocity components and the maximum temperature within the problem domain. As an outcome of this study, optimized grid sizes are selected, so as to achieve a trade-off between numerical accuracy and computational economy. For instance, a 40×5000 rectangular grid system is adopted to discretize a domain with an aspect ratio of $a = 10000$. It is revealed that a further refinement of the computational grids does not alter the accuracy of the final solutions to an appreciable extent. Convergence in the iterations is declared only when the following conditions are simultaneously satisfied:

(i) $\left|\frac{\phi-\phi_{old}}{\phi_{max}}\right| \leqslant 10^{-5}$, where ϕ stands for each scalar variable solved for at a grid point at the current iteration level, ϕ_{old} represents the corresponding value at the previous iteration level, and ϕ_{max} is the maximum value of the variable at the iteration level in the entire domain.

(ii) The overall energy balance within the computational domain is satisfied with an error of less than 1%.

With regard to the slip and jump boundary conditions, diffused reflections with full accommodation ($\sigma_v = 1$, $\sigma_T = 1$) [14] are considered.

Although the numerical solutions are obtained in dimensional forms for accommodating temperature-dependent thermo-physical properties, the results are parameterized with the aid of a representative value of the Rayleigh number (Ra), defined on the basis of the pertinent thermo-physical properties calculated with the ambient state as the reference, as follows: $Ra = \frac{\rho_\infty^2 c_{p\infty} g \beta_\infty D^3 (T_w - T_\infty)}{\mu_\infty k_\infty}$. The reference value of the Prandtl number, $Pr = \frac{\mu_\infty c_{p\infty}}{k_\infty}$, is taken to be 0.7, for all the numerical computations presented in this study.

3. Results and discussion

For validation of the numerical code employed for solving the physical problem under consideration, the fully developed velocity profiles, as obtained by simulating the present mathematical model, are compared with the analytical predictions of Chen and Weng [8], for $Ra = 100$ and $Kn = 0.1$, as depicted in Fig. 3. For convenience, only the velocity distributions over half-width of the channel are shown in the figure. The non-dimensional parameters adopted for plotting this figure are as follows: $x' = x/D$ and $v' = v/v_{ref}$ (where $v_{ref} = \mu_\infty/\rho_\infty D$). The present results are in excellent agreement with the corresponding analytical solutions [8] for fully developed flow conditions, as evident from Fig. 3.

Fig. 4 exhibits the variations in the dimensionless entrance length, Y_{eth} (which is the entrance length normalized with respect to the channel height) channel, as a func-

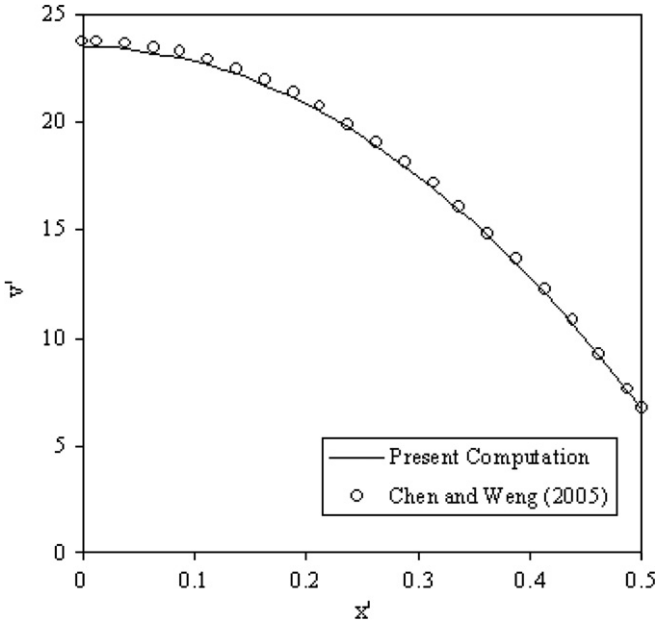

Fig. 3. A comparison of fully developed velocity profiles, as obtained from the present analysis and that reported in the work of Chen and Weng [8]. For obtaining these plots, $Ra = 100$ and $Kn = 0.1$ are taken.

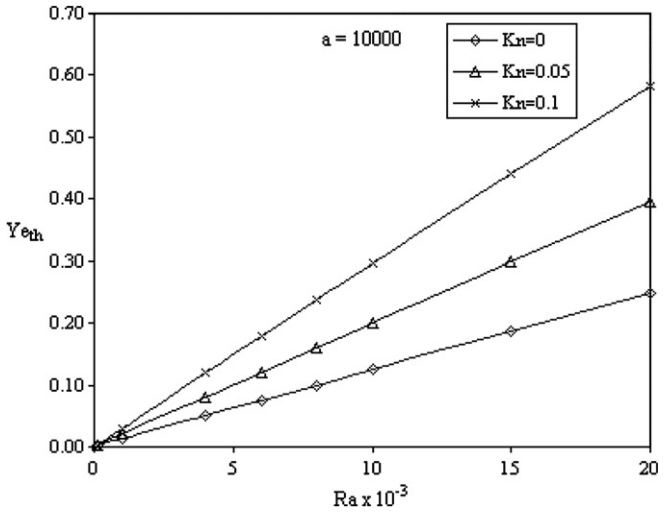

Fig. 4. Variations of thermal entrance length with *Ra*, for different values of *Kn*.

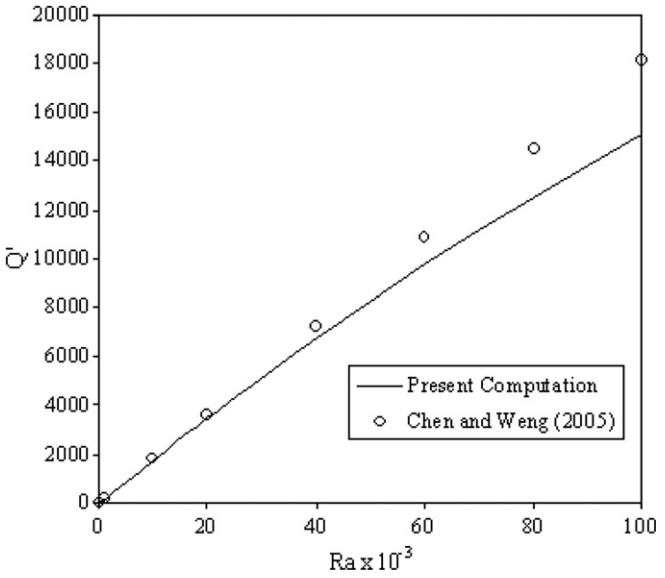

Fig. 5. Variations in the non-dimensional volume flow rate with *Ra*, for $Kn = 0.1$.

tion of *Ra*, for different values of *Kn*, corresponding to an aspect ratio of $H/D = a = 10^5$. It is important to note here that in the present case the hydrodynamic and the thermal entrance lengths are identical, since the condition of a hydrodynamically fully developed natural convection necessarily implies that the convection is also thermally fully developed [8]. It is apparent from Fig. 4 that with an increase in the value of *Ra*, the entrance region persists over a greater proportion of the channel height. The entrance length also increases with an increase in the value of *Kn*. This can be physically explained as follows. For a given thermal potential $(T_w - T_\infty)$ for free convection flow, the micro-scale effects, as manifested by the velocity slip and the temperature jump conditions at the walls, result in higher flow velocities, as compared to those in the no-slip regimes. This, in turn retards the growth of both hydrodynamic and thermal boundary layers, and thereby increases the entrance length.

Fig. 5 depicts the variation of the non-dimensional volume flow rate through the microchanel, $Q' = \int_0^1 \frac{v}{v_{ref}} dx'$, as a function of *Ra*. It is observed that there is a fairly good agreement between the present predictions and the results of Cheng and Wang [8], only for small values of *Ra*. The differences between these two predictions, however, become significantly more prominent for higher values of *Ra*. This can be attributed to the fact that while the work of Cheng and Wang [8] deals with a fully developed flow, the present work pertains to a flow comprising of both developing and developed regions. However, at low values of *Ra*, the developing flow region is much shorter in length, as compared to the total height of the channel (Fig. 4) and therefore, turns out to be inconsequential in altering the flow-rate predictions. On the other hand, the effects of the developing region become progressively more important for higher values of *Ra*, for which greater extents of the channel are characterized with the boundary layer growth. As a consequence, the resultant flow-rates are somewhat less than those predicted from the fully developed flow considerations made without accounting for the developing region.

Fig. 6 shows the variation of non-dimensional bulk mean temperature of the fluid, $\theta_b = \frac{T_b - T_\infty}{T_w - T_\infty}$ (where T_b is the bulk mean flow temperature) as a function of the non-dimensional channel height, $y' = y/D$, for a given value of *Ra*. It is observed that the bulk mean temperature approaches the wall temperature at axial locations where the flow has already become fully developed. It is further noticed that with an increase in *Kn*, the axial distance from the channel entrance to the location of this asymptotic merging becomes longer. This is because of the fact that at any given value of *Ra*, the entrance length is higher for flows with higher values of *Kn*, as apparent from Fig. 4.

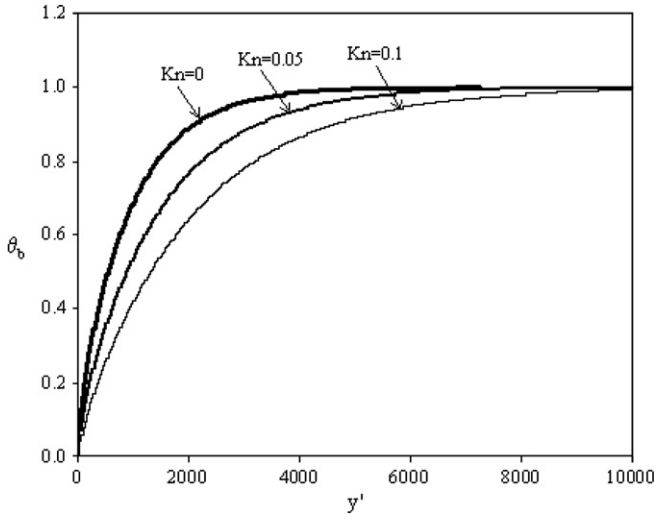

Fig. 6. Variations of non-dimensional bulk mean temperature of flow along the height of the channel, for different values of *Kn*, with $Ra = 10^5$ and $a = 10000$.

Fig. 7 shows the variations of the axially-averaged Nusselt number, $\overline{Nu}$, with Ra, for different values of Kn. It is observed from the figure that the $\overline{Nu}$ approaches zero in the limits of very small values of Ra, irrespective of the value of Kn. This is because of the fact that with lower values of Ra, the entrance region almost vanishes and the flow is virtually fully developed over the entire channel length. This also corroborates the fact that for fully developed natural convection, the Nusselt number asymptotically tends to zero for symmetric wall heating conditions, as reported in the literature [8]. However, at higher values of Ra, for which a fully developed flow is preceded by a considerable developing region, there occurs an increase in $\overline{Nu}$ with an increase in Kn. This enhancement in heat transfer with more prominent micro-scale effects can be physically explained as follows. Under an imposed pressure gradient due to thermal buoyancy effects, the mass flow rate turns out to be higher in presence of more prominent wall-slippage effects. This causes an enhancement in the rate of heat transfer. On the other hand, a temperature jump at the wall tends to decrease the local temperature gradients, and thereby reduces the rate of heat transfer between the wall and the fluid. The race between these two counterweighing effects eventually decides whether there would be an augmentation or a reduction in the rate of heat transfer in presence of wall-slip and temperature-jump effects. Under the present conditions, the influence of the increased mass flow rate on heat transfer becomes the predominant factor, and thus, an enhancement in the rate of heat transfer with increases in the value of Kn occurs. To obtain a more detailed picture of the variations in the Nusselt number, Fig. 8 is plotted, which depicts the variation in the local Nusselt number, Nu, along the height of the channel. It is observed that an initial steep fall in Nu is followed by a gradual decrease to an asymptotic value of zero in the fully developed region. The initial steep gradients in Nu can be attributed to the rapid growth of the thermal boundary layer for microchannel flows. With higher values of Kn, however, the boundary layer growth and a subsequent attainment of the fully developed conditions is somewhat delayed, as attributable to the wall slip effects.

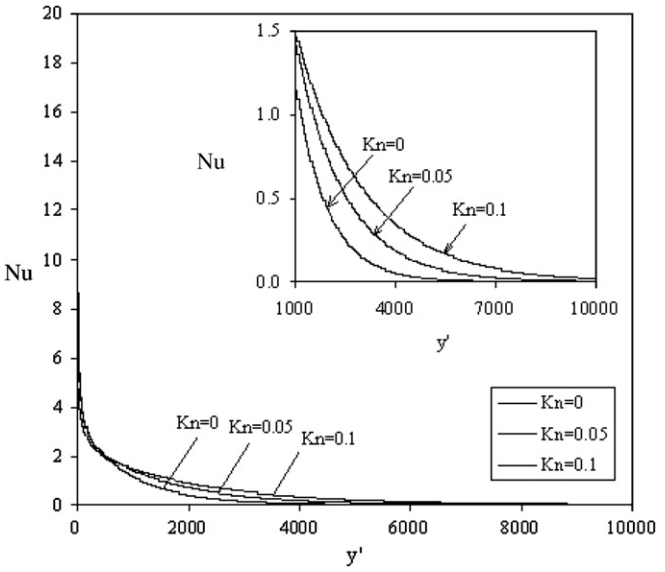

Fig. 8. Variations in local Nusselt number along the height of channel, for $Ra = 10^5$, with different values of Kn.

Fig. 9 summarizes the percentage enhancement in the value of $\overline{Nu}$, as attributable to the micro-scale effects on account of wall-slippage and temperature-jump conditions. An increase of 50–60% in the value of $\overline{Nu}$ for $Kn = 0.1$, and an increase of 25–30% in the value of $\overline{Nu}$ for $Kn = 0.05$ can be observed from the figure, within the range of the Ra values numerically studied here. Interestingly, there is a decli-

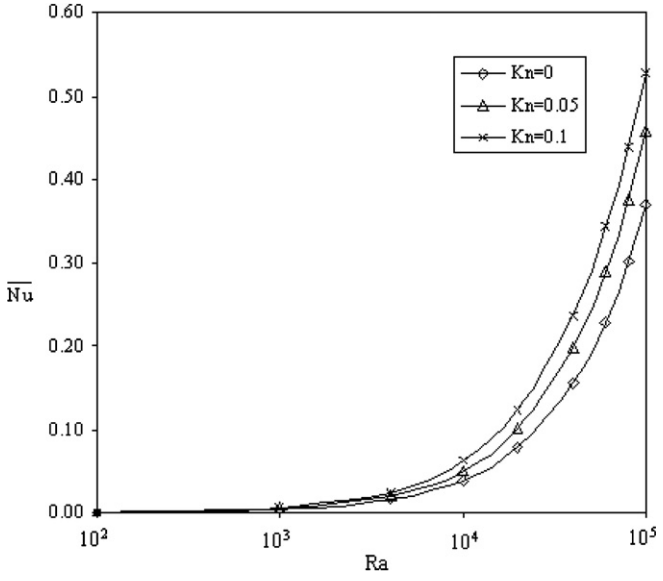

Fig. 7. Variations in $\overline{Nu}$ with Ra, for different values of Kn, with $a = 10000$.

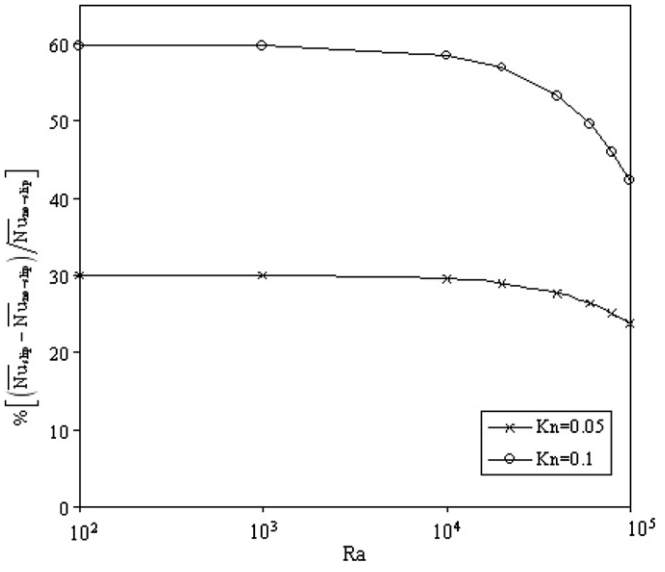

Fig. 9. Percentage variations in $\overline{Nu}$ for flows with slip and without slip, as a function of Ra, for different values of Kn.

nation in the percent enhancement in $\overline{Nu}$ at higher values of Ra. This can be attributed to the fact that the thermal boundary layer thickness is reduced at higher values at Ra, and therefore, the enhancement in $\overline{Nu}$ for micro-scale flows becomes significantly more important in the high Ra regimes.

4. Conclusions

Numerical computations have been performed to investigate the heat transfer characteristics in free convection gas flows in symmetrically heated vertical microchannels, comprising of both developing and the fully developed regions, under the conditions of large channel aspect ratios, with temperature-dependent thermo-physical properties. The results of micro-scale slip flows are compared with standard macro-scale flow predictions. The major observations from the present study can be summarized as follows:

(i) In case of micro-scale natural convection flows with velocity slip and temperature jump conditions at the walls, enhanced heat transfer rates are realized due to an increased mass flow rate and longer thermal entrance lengths, as compared to the classical macro-scale flow.
(ii) The proportionate enhancement in the average Nusselt number for the case of micro-scale flows becomes more prominent with higher values of Knudsen number. However, the relative augmentation in the rate of heat transfer due to micro-scale effects tends to get somewhat reduced for higher values of Rayleigh number.
(iii) For low values of Rayleigh number, the entrance region length is only a small fraction of the total channel and hence, the Nusselt number averaged over the channel height tends to zero, as reported in the literature for the cases of fully developed flows with symmetrical heating conditions. For higher values of Rayleigh number, however, the effects of developing length are non-trivial, and two counteracting heat transfer mechanisms need to be aptly taken into consideration for interpreting the averaged Nusselt number values.

References

[1] M. Gad-el-Hak, The fluid mechanics of microdevices – the freeman scholar lecture, J. Fluid Eng., ASME 121 (1999) 5–33.
[2] A. Beskok, G.E. Karniadakis, A model for flows in channels, pipes and ducts at micro and nano scales, Microscale Thermophys. Eng. 3 (1999) 43–77.
[3] A. Beskok, W. Trimmer, G.E. Karniadakis, Rarefaction and Compressibility Effects in Gas Microflows, J. Fluids Eng. 118 (3) (1996) 448–456.
[4] E.G.R. Eckert, R.M. Drake Jr., Analysis of Heat and Mass Transfer, McGraw-Hill, New York, 1972, pp. 467–486.
[5] E.H. Kennard, Kinetic Theory of Gases, McGraw-Hill, New York, 1938.
[6] M. Gad-el-Hak, Comments on critical view on new results in microfluid mechanics, Int. J. Heat Mass Transfer 46 (2003) 3941–3945.
[7] G.E. Karniadakis, A. Beskok, Microflows: Fundamentals and Simulation, Springer-Verlag, New York, 2002.
[8] C.-K. Chen, H.C. Weng, Natural convection in a vertical microchannel, J. Heat Transfer 127 (2005) 1053–1056.
[9] D.Y. Shang, B.X. Wang, Effect of variable thermophysical properties on laminar free convection of gas, Int. J. Heat Mass Transfer 33 (1990) 1387–1395.
[10] M. Gad-El-Hak, The MEMS Handbook, CRC Press, 2001.
[11] A. Bejan, Convection Heat Transfer, third ed., John Wiley & Sons, 1984, pp. 210.
[12] H.L. Stone, Iterative solution of implicit approximations of multidimensional partial differential equations, SIAM J. Numer. Anal. 5 (1968) 530.
[13] S.V. Patankar, Numerical Heat Transfer and Fluid Flow, McGraw-Hill, 1980.
[14] R.F. Barron, X. Wang, T.A. Ameel, R.O. Warrington, The graetz problem extended to slip flow, Int. J. Heat Mass Transfer 40 (1997) 1817–1823.